Research

Nonenzymatic Electrochemical Sensing of Hydrogen Peroxide Based on Gold Nanolayers Covered with Snow-like Nanoparticles

Rezvan Dehdari Vais, Hossein Heli*

Nanomedicine and Nanobiology Research Center, Shiraz University of Medical Sciences, Shiraz, Iran

*****Correspondence should be addressed to Hossein Heli, Nanomedicine and Nanobiology Research Center, Shiraz University of Medical Sciences, Shiraz, Iran; Tel: +987136282225; Fax: +987136281506; Email: hheli7@yahoo.com; heli@sums.ac.ir.**

ABSTRACT

Gold nanolayers covered with snow-like nanoparticles were firstly synthesized by the sonoelectrodeposition method at a high negative potential. The nanostructure was then applied to prepare a highly sensitive nonenzymatic sensor for hydrogen peroxide. The catalytic activity and sensitivity of the gold nanostructure toward the electroreduction of hydrogen peroxide was excellent without surface fouling and deterioration effects. The current related to the reduction of hydrogen peroxide rapidly and linearly depended on the concentration with a sensitivity of 0.24 A mol^{-1} dm^3 cm^{-2} and a detection limit of 7.9 μmol dm^{-3}. The present hydrogen peroxide sensor was fabricated by a simple preparation method without using any specific enzyme or reagent, with an excellent catalytic activity, high sensitivity and selectivity, long-term stability, and antifouling property.

Key words: Hydrogen peroxide, Electrocatalysis, Nonenzymatic sensor, Sonoelectrodeposition, 3D nanostructure.

1. INTRODUCTION

Hydrogen peroxide is an important intermediate compound in many biological reactions, and is employed as an antiseptic or disinfectant for medical and packaging purposes. It is widely used in industrial processes as a bleaching agent for cellulose, papers and fibers, in waste treatment as a deodorant, and in the semiconductor fabrication as a cleaning agent (1, 2). Therefore, development of sensitive and selective methods for hydrogen peroxide determination is important in food, and pharmaceutical, biomedical, clinical, industrial and environmental analyses (3-6). As for the hydrogen peroxide determination, enzymatic and protein-based biosensors have the disadvantages of instability of the enzymes or proteins, complex immobilization process and high costs. On the other hand, direct or mediated electrooxidation- or electroreduction-based sensors without using enzyme and protein have the advantages of simplicity, high sensitivity, fast response time, low cost and convenient operation. To attain these advantages, hydrogen peroxide electrochemical sensors have been fabricated using novel nanostructures of metals, metal-based composites, metal oxides, metal hexacyanoferrates and conducting polymers (7-11).

Nanostructured materials represent size- and shape-dependent properties, including chemical (re)activity resulting in the fabrication of highly sensitive electrochemical sensors (12). Therefore, the development of synthesis routes to prepare novel nanostructured materials with different sizes and shapes is highly desirable. Different nanostructures of gold have been applied to fabricate electrochemical sensors and biosensors including nanoparticles (13), nanowires (14), nanocomposite (15), nanorod (16), nanochains (17), and nanodots (18). Up to now, different electrochemical hydrogen peroxide sensors have also been fabricated based on gold nanostructures (11, 13, 14, 17, 18). However, due to the size and shape dependent properties of the gold nanostructures, there is a plenty room to fabricate nonenzymatic hydrogen peroxide sensors based on novel gold nanostructures. In this work, an amperometric hydrogen peroxide sensor was presented using gold nanolayers covered with snow-like nanoparticles.

2. MATERIALS AND METHODS

All chemicals used in this work were reagent grade from Merck or Sigma products and used without further purifications. A 100 mmol dm^{-3} phosphate buffer solution (PBS), pH=7.4 was prepared using NaH_2PO_4 and Na_2HPO_4. Doubly distilled water was used throughout the study. Electrochemical studies were performed in a conventional three-electrode cell powered by a μ-Autolab potentiostat/galvanostat, type III, FRA2 (The Netherlands) run by a computer through GPES 4.9 software. An Ag/AgCl/3 mol dm^{-3} KCl and a glassy carbon wire were used as the reference and counter electrodes, respectively. The working electrode was a gold disk (Au) electrode of 2 mm diameter modified by gold nanolayers covered by snow-like nanoparticles (nAu). Studies on the electrocatalytic reduction and determination of hydrogen peroxide were performed in PBS as the running electrolyte. PBS was used as the running electrolyte to mimic the physiological medium.

In order to prepare the modified (Au/nAu) electrode, the Au electrode was firstly polished on sand papers, and then on a polishing pad with 50 nm-alumina powder lubricated by glycerin. Polishing was continued to attain a mirror-like surface. The electrode was then cleaned by immersion in a 1:3 water/ethanol mixture and ultrasonication for 5 min in an ultrasound bath. The electrode was further electropolished by immersion in a 500 mmol L^{-1} H_2SO_4 solution and applying cyclic potentials in the range of cathodic and anodic edges of the electrolyte for 25 consecutive cycles. The Au electrode was then placed in the cell containing 5 mmol dm^{-3} $HAuCl_4$ + 0.5 mol dm^{-3} KCl. nAu was sonoelectrodeposited at a potential of -1800 mV for a duration of 300 s, while during the electrodeposition, the synthesis solution and the Au electrode surface were irradiated by ultrasound waves of 45-W power. Au/nAu electrode was then rinsed thoroughly with distilled water. In order to obtain information about the morphology and size of the electrodeposited gold nanostructure, field emission scanning electron microscopy (FESEM) was performed by Zeiss, Sigma-IGMA/VP (Germany). Amperometric measurements for hydrogen peroxide quantitation were performed at -200 mV in a magnet-stirring solution wherein the solution was rapidly homogenized after each hydrogen peroxide injection. To investigate the capability of the Au/nAu electrode to detect hydrogen peroxide in real samples, two river water samples taken from different local rivers were analyzed. The water samples were put intact for two days to settle. After that, the amperometric responses of the Au/nAu electrode were measured by hydrogen peroxide addition of known concentrations to the samples. All studies were carried out at room temperature.

3. RESULTS AND DISCUSSION

Figure 1 represents a FESEM image of the electrodeposited gold surface. The nanostructure has a complex morphology, and at low magnification, comprises clung nanolayers which are partly covered by snow-like nanoparticles. Electrodeposition of gold nanolayers covered with snow-like nanoparticles occurred under nonequilibrium conditions due to the correlations between the newly deposited species and their neighboring position during the mass transport process (19). In the formation of this structure, both irradiation of ultrasound and hydrogen co-evolution play key roles, and elimination of ultrasound irradiation, or application of less negative potentials lead to formation of other gold structures.

Figure 1. A FESEM image of the electrodeposited gold surface

Figure 2 shows cyclic voltammograms of Au and Au/nAu electrodes recorded in PBS in the absence and presence of 1.0 mmol dm^{-3} hydrogen peroxide. The reduction of hydrogen peroxide on the Au/nAu electrode occurred at lower potentials with a higher rate, compared to the Au electrode. Both aspects are highly important for development of a determination method of hydrogen peroxide with high sensitivity without interference from other substances. In order to compare the surface areas of the Au and Au/nAu electrodes and their roughness factors, cyclic voltammograms of the Au/nAu electrode at different potential sweep rates were recorded in a solution of KCl (0.5 mol dm^{-3}) containing K$_4$[Fe(CN)$_6$] (0.5 mmol dm^{-3}), as a redox probe. The real surface area was obtained from the Randles-Sevcik equation (20) and the value of 7.60×10^{-6} cm s^{-1} for the diffusion coefficient of [Fe(CN)$_6$]$^{4-}$ (21) (Supplementary material S1). Based on the results, the real surface area of the Au and Au/nAu electrodes was obtained as 0.058 and 0.73 cm^2, respectively. Regarding the geometric surface area of the electrodes (equal to 0.031 cm^2), the roughness factors were obtained as 1.86 and 23.19 for Au and Au/nAu electrodes, respectively.
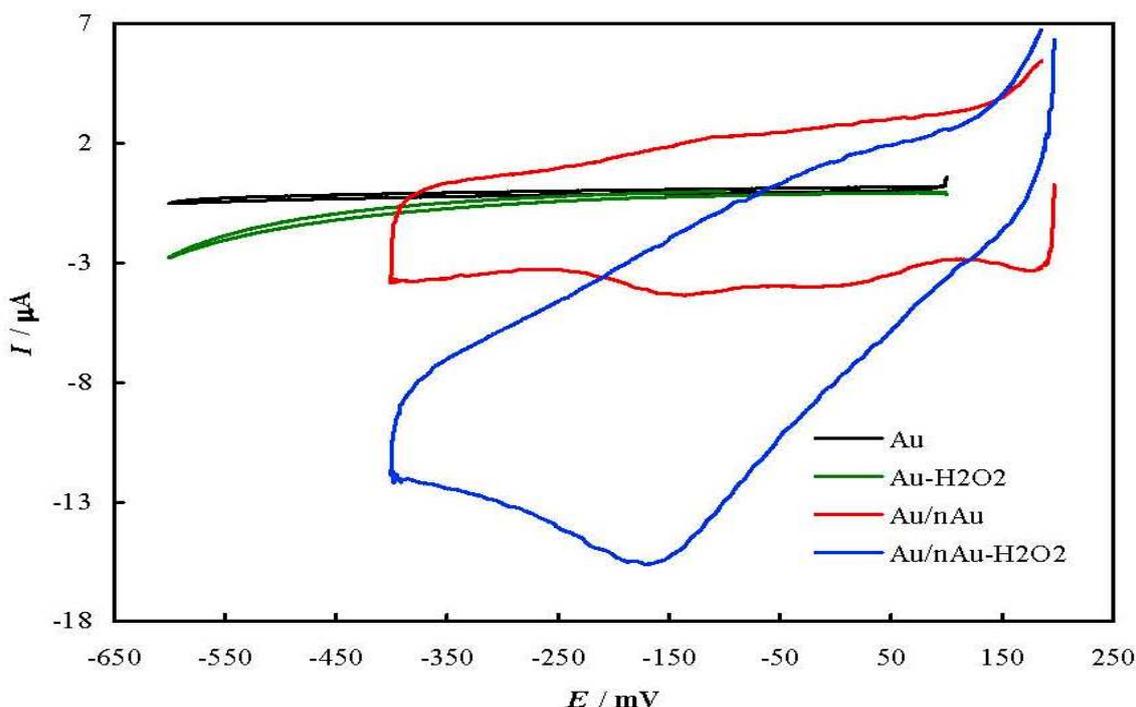
Figure 2. Cyclic voltammograms of Au and Au/nAu electrodes recorded in PBS in the absence and presence of 1.0 mmol dm^{-3} hydrogen peroxide. The potential sweep rate was 50 mV s^{-1}

On the other hand, the potential of the hydrogen peroxide electroreduction in the voltammograms of Fig. 2 on the Au/nAu electrode is more positive, and the corresponding current at the potential of -170 mV (peak potential of hydrogen peroxide electroreduction on the Au/nAu electrode surface) is ~58 times higher, compared to the Au electrode. While the active surface area of the Au/nAu electrode is about ~12.6 times higher than the Au electrode. The results indicate that hydrogen peroxide is electroreduced on the Au/nAu electrode from both kinetics and thermodynamics points of views. The acceleration of electroreduction of hydrogen peroxide by the Au/nAu electrode can be related to the change in the valence band density of states of gold nanostructure (22) which comprises different reactive facets (23). In addition, mass transport regime can be altered (24) by the high coverage of gold clusters. It can also be added that the (re)activity of facets and steps in the nanostructures is different with smooth surfaces (25), and it can alter the reaction kinetics. In order to develop a sensor for detection of hydrogen peroxide based on the Au/nAu electrode, the amperometry technique was employed. Figure 3 shows typical amperometric signals during the successive addition of hydrogen peroxide to PBS at a working potential of -200 mV. Gentle magnetic stirring for a few seconds was needed to homogenize the solution after each addition.
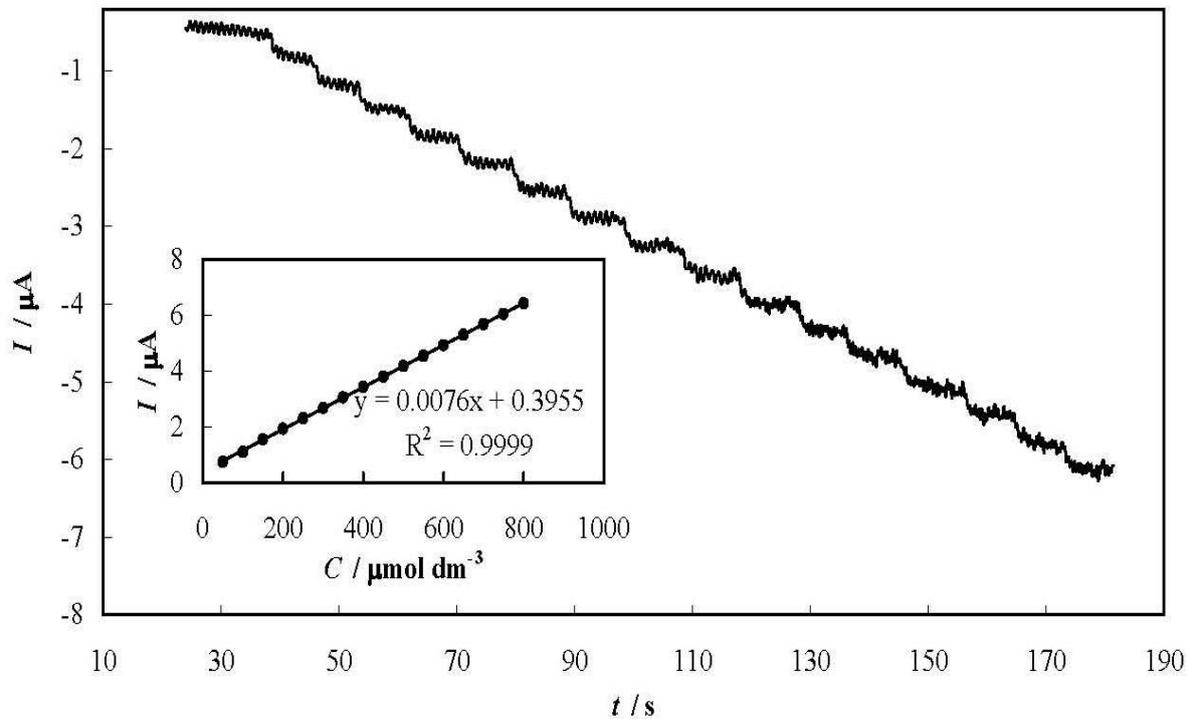
Figure 3. Typical amperometric signals during the successive addition of hydrogen peroxide to PBS at the potential of -200 mV. Inset: The corresponding calibration curve

The Au/nAu electrode responded rapidly and linearly to the hydrogen peroxide concentration (Figure 3, inset). The limits of detection (LOD) and quantitation (LOQ) of the method were calculated as 3SD/m and 10SD/m, respectively, where SD is the standard deviation of the blank signal and m is the slope of the calibration curve (26). The determined parameters for the calibration curve of hydrogen peroxide were obtained as LOD=7.9 μmol dm^{-3}, LOQ=26.3 μmol dm^{-3}, RSD (relative SD)=4.25%, sensitivity=0.24 A mol^{-1} dm^3 cm^{-2}, and a linear range of 50-800 μmol dm^{-3}. A comparison of some different hydrogen peroxide sensors is presented in Table 1, showing that the present amperometric sensor based on gold nanolayers covered with snow-like nanoparticles has better or comparable characteristics. Long-term amperometric response of the Au/nAu electrode to 50 μmol dm^{-3} hydrogen peroxide for 20 min is presented in Figure 4 A. The response remained stable during the measurement (<5% fluctuation in the current). This indicates that no fouling or blocking of the electrode surface occurred, and the electrode showed high stability and strong mediation properties for amperometric measurements of hydrogen peroxide.

Table 1. Comparison of some different hydrogen peroxide sensors

Electrode	Potential / V	Sensitivity / A mol^{-1} dm^3 cm^{-2}	LOD / μmol dm^{-3}	Linear range / μmol dm^{-3}	Reference
Ag NPs	-0.3 [b]	-	33.9	100-180000	(27)
Fe$_3$O$_4$-Ag	-0.5 [b]	0.012	1.2	1.2-3500	(28)
Ppy-Cu/Au	-0.3 [a]	-	2.3	7.0-4300	(29)
HRP-sol gel	-0.25[b]	-	12.89	0.013-10.6	(30)
Ag-SWCNTs	-0.3 [a]	1.092	2.76	16-18000	(31)
Ag NPs/PoPD	-0.5 [a]	-	1.5	6.0-67300	(32)
Pt Nanoflower	-0.2 [b]	-	60	100-900	(33)
Pt-carbon paste	0.8 [b]	-	5	-	(34)
PtPd/MWCNTs	0.25 [a]	-	1.2	2.5-125	(35)
Pt/MWCNTs-PANI	-0.25 [a]	-	2.0	7.0-2500	(36)
Pt NPs-MWCNTCs	-0.4 [b]	-	1.23	5-2000	(37)
Se/Pt nanocomposites	0.0 [b]	-	3.1	0.01-15	(38)
Pt NPs-PPy nanowires	-0.3 [a]	-	1.2	3.5-9900	(39)
Macroporous Au/Pt NPs	0.1 [b]	0.264	50	-	(40)
Graphene/Au NPs/chitosan	-0.2 [b]	-	-	0.2-4.2	(41)
Pt NPs-micro carbon pillars	-0.4 [b]	1.28-1.75	9.6-17.7	to 7000	(42)
Platinum hierarchical nanoflowers	0.21 [b]	1.39	1.05	10-400	(14)
Au nanolayers covered with snow-like nanoparticles	-0.2 [b]	0.24	7.9	50-800	This work

a Potential versus SCE.
b potential versus Ag/AgCl

SWCNT: Single wall carbon nanotube
PoPD: Poly(o-phenylene diamine)
MWCNTs: Multi wall carbon nanotube

Abbreviations:
CNT: carbon nanotube
NPs: Nanoparticles
HRP: Horseradish peroxidase

PANI: Polyaniline
PPy: Polypyrrole

In order to inspect the selectivity of the Au/nAu electrode, the interference effects of some common biological interferences of dopamine, ascorbic acid, glucose and uric acid were evaluated and are shown in Figure 4 B. No electrochemical interference was observed for these compounds due to electrocatalytic nature of the gold nanostructure toward the electroreduction of hydrogen peroxide at the applied potential. In order to inspect the capability of the Au/nAu electrode in detection of hydrogen peroxide in real samples, river samples were analyzed by amperometry. The determined parameters for

the calibration curve of hydrogen peroxide in a typical river water sample are as LOD=10.2 μmol dm^{-3}, LOQ=34.1 μmol dm^{-3}, RSD=4.83%, sensitivity=0.20 A mol^{-1} dm^3 cm^{-2}, and a linear range of 50-800 μmol dm^{-3}. In addition, the recovery results of hydrogen peroxide determination in two river samples were obtained as 98.85% and 98.11%. Based on the results, the electrode demonstrated an excellent sensing capability in detecting hydrogen peroxide in real samples.
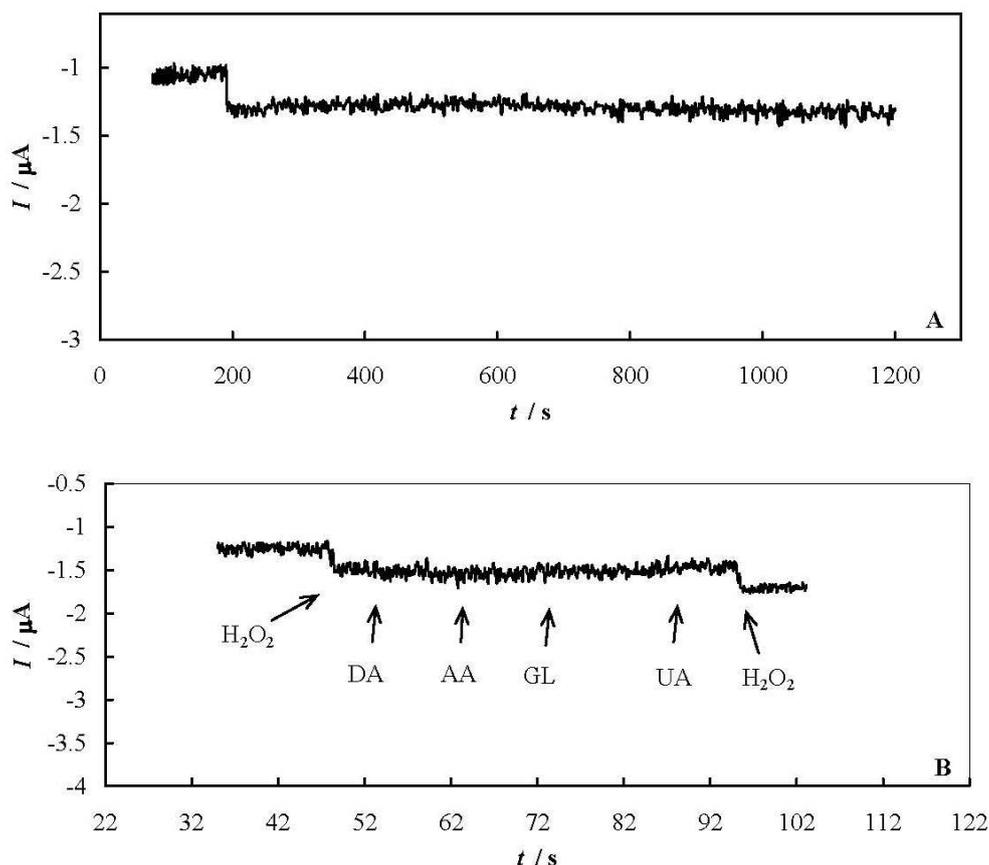
Figure 4. (A) Lon-term amperometric response of the Au/nAu electrode to 50 μmol dm^{-3} hydrogen peroxide for 20 min (B) Typical amperometric signals for 50 μmol dm^{-3} hydrogen peroxide, dopamine, ascorbic acid, glucose and uric acid to PBS. (UA: Uric acid, DA: Dopamine, AA: Ascorbic acid). The potential was -200 mV.

In order to inspect the durability and long-term stability of the Au/nAu electrode, amperometric measurements were performed in five successive days, and it was found that the currents changed slightly (<5%). In addition, the electrode was stored in distilled water when not in use and retained its activity for at least five weeks.

4. CONCLUSION

A sonoelectrodeposition method at a highly negative potential was developed for the synthesis of gold nanolayers covered with snow-like nanoparticles. It seems that hydrogen co-evolution played a major role in the synthesis of this nanostructure, and the procedure might be applied to the synthesis of other noble metals. This gold nanostructure showed an enhanced electrocatalytic activity towards the reduction of hydrogen peroxide without

interfering effect. The sensor showed remarkable electrocatalytic activity, stable response and high sensitivity toward hydrogen peroxide.

AUTHORS CONTRIBUTION

This work was carried out in collaboration among all authors.

CONFLICT OF INTEREST

The authors declared no potential conflicts of interests with respect to the authorship and/or publication of this paper.

REFERENCES

1. Gould G, Irene E. The influence of silicon surface cleaning procedures on silicon oxidation. Journal of Electrochemical Society. 1987;134(4):1031-1033.
2. Schumb WC, Satterfield CN, Wentworth RL. Hydrogen peroxide. 1955.
3. Yao S, Xu J, Wang Y, Chen X, Xu Y, Hu S. A highly sensitive hydrogen peroxide amperometric sensor based on MnO 2 nanoparticles and dihexadecyl hydrogen phosphate composite film. Analytica chimica acta. 2006;557(1):78-84.
4. Kriz K, Kraft L, Krook M, Kriz D. Amperometric determination of L-lactate based on entrapment of lactate oxidase on a transducer surface with a semi-permeable membrane using a SIRE technology based biosensor. Application: tomato paste and baby food. Journal of agricultural and food chemistry. 2002;50(12):3419-24.
5. Vione D, Maurino V, Minero C, Borghesi D, Lucchiari M, Pelizzetti E. New processes in the environmental chemistry of nitrite. 2. The role of hydrogen peroxide. Environmental science & technology. 2003;37(20):4635-41.
6. You T, Niwa O, Tomita M, Hirono S. Characterization of platinum nanoparticle-embedded carbon film electrode and its detection of hydrogen peroxide. Analytical chemistry. 2003;75(9):2080-5.
7. Heli H, Sattarahmady N, Vais RD, Mehdizadeh A. Enhanced electrocatalytic reduction and highly sensitive nonenzymatic detection of hydrogen peroxide using platinum hierarchical nanoflowers. Sensors and Actuators B: Chemical. 2014;192:310-6.
8. Fang Y, Zhang D, Qin X, Miao Z, Takahashi S, Anzai J-i, et al. A non-enzymatic hydrogen peroxide sensor based on poly (vinyl alcohol)–multiwalled carbon nanotubes–platinum nanoparticles hybrids modified glassy carbon electrode. Electrochimica Acta. 2012;70:266-71.
9. Heli H, Pishahang J. Cobalt oxide nanoparticles anchored to multiwalled carbon nanotubes: Synthesis and application for enhanced electrocatalytic reaction and highly sensitive nonenzymatic detection of hydrogen peroxide. Electrochimica Acta. 2014;123:518-26.
10. Chen W, Cai S, Ren Q-Q, Wen W, Zhao Y-D. Recent advances in electrochemical sensing for hydrogen peroxide: a review. Analyst. 2012;137(1):49-58.
11. Narang J, Chauhan N, Pundir C. A non-enzymatic sensor for hydrogen peroxide based on polyaniline, multiwalled carbon nanotubes and gold nanoparticles modified Au electrode. Analyst. 2011;136(21):4460-6.
12. Zhu C, Yang G, Li H, Du D, Lin Y. Electrochemical sensors and biosensors based on nanomaterials and nanostructures. Analytical chemistry. 2014;87(1):230-49.
13. Ma X, Chen M. Electrochemical sensor based on graphene doped gold nanoparticles modified electrode for detection of diethylstilboestrol. Sensors and Actuators B: Chemical. 2015;215:445-50.
14. Shi L, Chu Z, Liu Y, Jin W. Facile fabrication of a three-dimensional gold nanowire array for high-performance electrochemical sensing. Journal of Materials Chemistry B. 2015;3(16):3134-40.
15. Zheng Y, Wang A, Lin H, Fu L, Cai W. A sensitive electrochemical sensor for direct phoxim detection based on an electrodeposited reduced graphene oxide–gold nanocomposite. RSC Advances. 2015;5(20):15425-30.
16. Bai W, Huang H, Li Y, Zhang H, Liang B, Guo R, et al. Direct preparation of well-dispersed graphene/gold nanorod composites and their application in electrochemical sensors for determination of ractopamine. Electrochimica Acta. 2014;117:322-8.
17. Chen S, Ma L, Yuan R, Chai Y, Xiang Y, Wang C. Electrochemical sensor based on Prussian blue nanorods and gold nanochains for the determination of H2O2. European Food Research and Technology. 2011;232(1):87-95.
18. El-Said WA, Choi J-W. Electrochemical Biosensor consisted of conducting polymer layer on gold nanodots patterned Indium Tin Oxide electrode for rapid and simultaneous determination of purine bases. Electrochimica Acta. 2014;123:51-7.
19. Barabási A-L, Stanley HE. Fractal concepts in surface growth: Cambridge university press; 1995.
20. Li J, Yuan R, Chai Y, Che X, Li W, Zhong X. Nonenzymatic glucose sensor based on a glassy carbon electrode modified with chains of platinum hollow nanoparticles and porous gold nanoparticles in a chitosan membrane. Microchimica Acta. 2011;172(1-2):163-9.
21. Yuan J, Wang K, Xia X. Highly ordered platinum-nanotube arrays for amperometric glucose sensing. Advanced Functional Materials. 2005;15(5):803-9.
22. Guczi L, Petö G, Beck A, Frey K, Geszti O, Molnár G, et al. Gold nanoparticles deposited on SiO2/Si (100): Correlation between size, electron structure, and activity in CO oxidation. Journal of the American Chemical Society. 2003;125(14):4332-7.
23. Wain AJ. Imaging size effects on the electrocatalytic activity of gold nanoparticles using scanning electrochemical microscopy. Electrochimica Acta. 2013;92:383-91.
24. Campbell FW, Belding SR, Baron R, Xiao L, Compton RG. Hydrogen peroxide electroreduction at a silver-nanoparticle array: investigating nanoparticle size and coverage effects. The Journal of Physical Chemistry C. 2009;113(21):9053-62.
25. Hernandez J, Solla-Gullon J, Herrero E. Gold nanoparticles synthesized in a water-in-oil microemulsion: electrochemical characterization and effect of the surface structure on the oxygen reduction reaction. Journal of Electroanalytical Chemistry. 2004;574(1):185-96.
26. Miller JC, Miller JN. Statistics for analytical chemistry. 1988.
27. Lu W, Liao F, Luo Y, Chang G, Sun X. Hydrothermal synthesis of well-stable silver nanoparticles and their application for enzymeless hydrogen peroxide detection. Electrochimica Acta. 2011;56(5):2295-8.
28. Liu Z, Zhao B, Shi Y, Guo C, Yang H, Li Z. Novel nonenzymatic hydrogen peroxide sensor based on iron oxide–silver hybrid submicrospheres. Talanta. 2010;81(4):1650-4.
29. Zhang T, Yuan R, Chai Y, Li W, Ling S. A novel nonenzymatic hydrogen peroxide sensor based on a polypyrrole nanowire-copper nanocomposite modified gold electrode. Sensors. 2008;8(8):5141-52.
30. Chen H, Dong S. Direct electrochemistry and electrocatalysis of horseradish peroxidase immobilized in sol–gel-derived ceramic–carbon nanotube nanocomposite film. Biosensors and Bioelectronics. 2007;22(8):1811-5.
31. Bui M-PN, Pham X-H, Han KN, Li CA, Kim YS, Seong GH. Electrocatalytic reduction of hydrogen peroxide by silver particles patterned on single-walled carbon nanotubes. Sensors and Actuators B: Chemical. 2010;150(1):436-41.
32. Wang L, Zhu H, Song Y, Liu L, He Z, Wan L, et al. Architecture of poly (o-phenylenediamine)–Ag nanoparticle composites for a hydrogen peroxide sensor. Electrochimica Acta. 2012;60:314-20.
33. Wan J, Wang W, Yin G, Ma X. Nonenzymatic H2O2 sensor based on Pt nanoflower electrode. Journal of Cluster Science. 2012;23(4):1061-8.
34. Wang J, Naser N, Angnes L, Wu H, Chen L. Metal-dispersed carbon paste electrodes. Analytical Chemistry. 1992;64(11):1285-8.
35. Chen K-J, Pillai KC, Rick J, Pan C-J, Wang S-H, Liu C-C, et al. Bimetallic PtM (M= Pd, Ir) nanoparticle decorated multi-walled carbon nanotube enzyme-free, mediator-less amperometric sensor for H 2 O 2. Biosensors and Bioelectronics. 2012;33(1):120-7.
36. Zhong H, Yuan R, Chai Y, Zhang Y, Wang C, Jia F. Non-enzymatic hydrogen peroxide amperometric sensor based on a glassy carbon electrode modified with an MWCNT/polyaniline composite film and platinum nanoparticles. Microchimica Acta. 2012;176(3-4):389-95.
37. Niu X, Zhao H, Chen C, Lan M. Platinum nanoparticle-decorated carbon nanotube clusters on screen-printed gold nanofilm electrode for enhanced electrocatalytic reduction of hydrogen peroxide. Electrochimica Acta. 2012;65:97-103.
38. Li Y, Zhang J-J, Xuan J, Jiang L-P, Zhu J-J. Fabrication of a novel nonenzymatic hydrogen peroxide sensor based on Se/Pt nanocomposites. Electrochemistry Communications. 2010;12(6):777-80.
39. Li J, Yuan R, Chai Y, Zhang T, Che X. Direct electrocatalytic reduction of hydrogen peroxide at a glassy carbon electrode modified with polypyrrole nanowires and platinum hollow nanospheres. Microchimica Acta. 2010;171(1-2):125-31.
40. Lee YJ, Park JY, Kim Y, Ko JW. Amperometric sensing of hydrogen peroxide via highly roughened macroporous Gold-/Platinum nanoparticles electrode. Current Applied Physics. 2011;11(2):211-6.
41. Shan C, Yang H, Han D, Zhang Q, Ivaska A, Niu L. Graphene/AuNPs/chitosan nanocomposites film for glucose biosensing. Biosensors and bioelectronics. 2010;25(5):1070-4.
42. Su J, Gao F, Gu Z, Pien M, Sun H. A novel 3-D fabrication of platinum nanoparticles decorated micro carbon pillars electrode for high sensitivity detection of hydrogen peroxide. Sensors and Actuators B: Chemical. 2013;181:57-64.